

## An on-line TDC-312 computer-controlled neutron diffractometer

A SEQUEIRA, S N MOMIN, H RAJAGOPAL,

J N SONI, R CHIDAMBARAM,

DILIP KUMAR\*, A RAMANA RAO\* and V M GOPU\*

Neutron Physics Section, Bhabha Atomic Research Centre, Bombay 400 085

\*Computer Group, Electronics Corporation of India Limited, Hyderabad 500 762

MS received 12 September 1977

**Abstract.** The design and fabrication of an indigenous on-line computer controlled four-circle neutron diffractometer at the CIRUS reactor in Trombay are described. The diffractometer has an 18 in dia full-circle crystal-orienter which is sturdy enough to carry a cryostat. Three crystal orientation angles  $\chi$ ,  $\phi$  and  $\omega$  and the detector angle  $2\theta$  can be set to an accuracy of  $0.01^\circ$ . The four angle shafts are driven through precision worm-gears by SCR-controlled DC motors and their instantaneous positions sensed by optical digitizers. The diffractometer is interfaced to an ECIL TDC-312 computer system consisting of the CPU with 4K-memory, ASR-35 teletype, X-Y plotter and the digital input/output system (DIOS). The DIOS which operates under program control is a real-time peripheral device used to exchange information in digital form between the computer and the diffractometer. A software package consisting of over 40 user-oriented teletype commands has been developed for on-line control and automatic data-acquisition.

**Keywords.** Computer controlled diffractometer; four-circle neutron diffractometer; diffractometer control software.

### 1. Introduction

The study of crystal and molecular structures by x-ray and neutron diffraction techniques has been one of the most fruitful scientific activities in recent years. An important factor leading to the success of these studies has been the use of on-line computers which have removed the drudgery of having to record manually the data from thousands of routine and repetitive measurements that are usually associated with typical diffraction experiments. On-line computers have enabled rapid and accurate data acquisition and processing, precise and reproducible parameter settings and have greatly enhanced the flexibility of diffraction experiments. Backed with suitable auxiliary memory and peripherals, the on-line computers have also been used for visual display of crystal structures and other computer graphics (Willoughby *et al* 1974). In this paper an indigenous on-line computer-controlled four-circle neutron diffractometer designed and commissioned more than an year back at the CIRUS reactor in Trombay is described. The system consists of a TDC-312 computer with 4K memory, an ASR-35 teletype, an X-Y plotter and a digital input/output system (DIOS) which serves as an interface between the computer and the diffractometer.

## 2. The four-circle diffractometer

The four-circle diffractometer has now become a standard instrument for recording single crystal diffraction data (Arndt and Willis 1966; Busing *et al* 1968). It enables rotation of the crystal about the three Eulerian axes  $\chi$ ,  $\phi$  and  $\omega$  and the rotation of the detector about the  $2\theta$ -axis as indicated schematically in figure 1. The axis of the  $\phi$ -circle is normal to the horizontal axis of the  $\chi$ -circle and rotates about the latter. The  $\phi$ - and  $\chi$ -circle assembly rotates as a whole about the vertical axis of the  $\omega$ -circle which is coincident with the counter axis. The sample crystal is located on the  $\phi$ -axis at the centre of the  $\chi$ -circle. The diffractometer could be used either in the 'symmetrical setting' or in the 'unsymmetrical' setting (Arndt and Willis 1966). In the symmetrical setting, by rotating about the  $\phi$ -circle, the scattering vector (or the reciprocal lattice vector corresponding to the reflecting plane) is brought into the plane of the  $\chi$ -circle which is in the bisecting position between the incident and the scattered beams. The reciprocal vector is then brought to the horizontal Bragg setting by rotating about the  $\chi$ -circle. The bisecting position of the  $\chi$ -circle is maintained by means of a  $\theta$ - $2\theta$  half angling system or by setting  $\omega = \theta$ . In the nonsymmetrical setting the  $\chi$ -circle is not in the bisecting position but makes an angle with the scattering vector. This angle enters the calculations of the setting angles and determines the azimuthal orientation of the reflecting plane. The calculation of the setting angles is generally carried out following methods suggested by Busing and Levy (1967).

Any reciprocal lattice vector  $\mathbf{h}$  ( $hkl$ ) can also be described in various cartesian coordinate systems. For example, if  $\mathbf{h}_c$  is the vector which describes  $\mathbf{h}$  in a crystal cartesian system, we can write

$$\mathbf{h}_c = \mathbf{B} \mathbf{h} \quad (1)$$

where  $\mathbf{B}$  is a transformation matrix determined by the cell parameters. Similarly, if  $\mathbf{h}_\phi$ ,  $\mathbf{h}_\chi$ ,  $\mathbf{h}_\omega$  and  $\mathbf{h}_\theta$  are the vectors which define  $\mathbf{h}$  in cartesian systems attached to the  $\phi$ -,  $\chi$ -,  $\omega$ - and  $\theta$ -circles respectively, then we can write

$$\mathbf{h}_\phi = \mathbf{U} \mathbf{h}_c \quad (2)$$

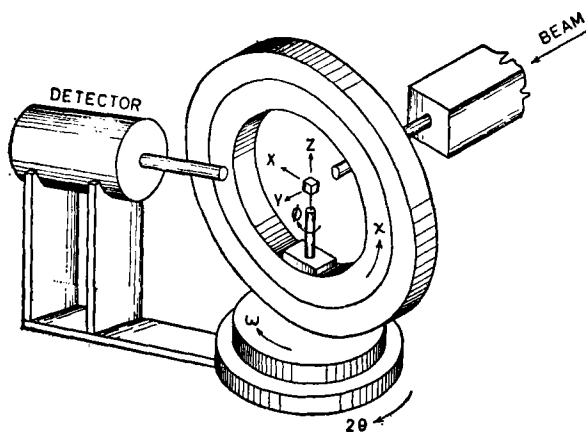
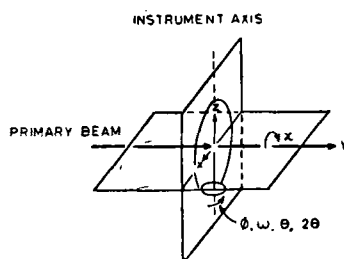


Figure 1. Schematic of the four circle geometry



The instrument with all angles set to zero. The coordinate axes are those of the  $\phi$ -axis,  $\chi$ -axis,  $\omega$ -axis,  $\theta$ -axis,  $2\theta$ -axis, and laboratory systems which are all coincident under these conditions.

Figure 2. The coordinate axes of the diffractometer

where  $\mathbf{U}$  is the orientation matrix determined by the orientation of the crystal mounted on the  $\phi$ -axis.

The  $\phi$ -,  $\chi$ -,  $\omega$ - and  $\theta$ - axes systems are supposed to be coincident with the laboratory system when all the instrument angles are set at their zero value. The latter has its  $y$ -axis along the incident beam and the  $z$ -axis along the vertical as shown in figure 2. Hence, we can have the following transformations:

$$\begin{aligned} \mathbf{h}_\chi &\underset{\cong}{=} \phi \mathbf{h}_\phi \\ \mathbf{h}_\omega &\underset{\cong}{=} \chi \mathbf{h}_\chi \\ \mathbf{h}_\theta &\underset{\cong}{=} \Omega \mathbf{h}_\omega \end{aligned} \quad (3)$$

where  $\phi$ ,  $\chi$  and  $\Omega$  are orthogonal matrices. Combining eqs (1), (2) and (3)

$$\mathbf{h}_\theta = \underset{\cong}{\Omega} \underset{\cong}{\chi} \underset{\cong}{\phi} \mathbf{U} \mathbf{B} \mathbf{h}. \quad (4)$$

At the Bragg condition

$$\mathbf{h}_\theta = \pm \begin{bmatrix} d^* \\ 0 \\ 0 \end{bmatrix} \underset{\cong}{=} \underset{\cong}{\Omega} \underset{\cong}{\chi} \underset{\cong}{\phi} \mathbf{U} \mathbf{B} \mathbf{h} \quad (5)$$

Setting angles for any reflection  $\mathbf{h}$  can be calculated using the above equation if  $\mathbf{U}$  and  $\mathbf{B}$  are known. The latter can in turn be calculated if the optimised setting angle for two reflections and the cell constants are known.

The present diffractometer which is set up at the beam hole E-19 of the CIRUS reactor consists of an 18 in. dia full  $\chi$ -circle on which the  $\phi$ -circle assembly is carried along with its drive and angle tracking system. It has been aligned such that the  $\chi$ - and the  $\phi$ -axis intersect orthogonally within a tolerance of 40 microns and an estimated tilt of  $0.03^\circ$ , with the point of intersection remaining on the  $\omega$ - and the  $2\theta$ -axes within the same tolerance. A photograph of the diffractometer\* is shown in figure 3.

\* Fabricated in Physics Group Workshop

Table 1. The monochromator and collimation parameters.

	Horizontal (FWHM) <sup>o</sup>	Vertical (FWHM) <sup>o</sup>
Primary in-pile collimation ( $\alpha_0$ )	0.72	1.40
Secondary collimation ( $\alpha_1$ )	1.25	1.75
Tertiary collimation ( $\alpha_2$ ) (sample to detector)	2.4	3.5
Monochromator mosaic spread	0.40	—
Monochromator take-off	19°	—

The (111) plane of a pressed doped germanium crystal has been used as the monochromator in transmission geometry. The present wavelength of the monochromatic beam is 1.035 Å and the estimated flux at the sample is  $6 \times 10^5$  neutrons/cm<sup>2</sup>/sec.

A 12 in. long, 1½ in. dia, B F<sub>3</sub> counter\*\* (at 75 cm gas pressure with 85% enrichment in B<sup>10</sup>) surrounded by a ¾ in. thick sheath of B<sub>4</sub>C followed by a 6 in. thick layer of borated paraffin is used 'end-on' as the neutron detector. It is preceded by a 10 in. long collimator carrying an insert of variable aperture. The designs of the detector and the monochromator shields are similar to those of an earlier instrument described elsewhere (Momin *et al* 1974).

The monochromator and the collimation parameters of the diffractometer are given in table 1.

### 3. The angle drive and tracking system

A basic requirement for on-line control of the diffractometer is a reliable drive system for its four angles  $\phi$ ,  $\chi$ ,  $\omega$  and  $2\theta$ . The shafts of these four angles are worm-driven using a gear ratio of 180 : 1 for the  $\phi$ -angle and 360 : 1 for the other three angles. Each drive is operated by a dc motor attached to one end of the worm shaft through an electromagnetic clutch which enables the motor to be decoupled for manual operation. The other end of the worm shaft is connected (via a 1 : 2 spur gear for the  $\phi$ -shaft and directly for the others) to a digitizer† which generates 100 pulses and a 'degree reference' pulse per shaft revolution. This enables positioning accuracies of 0.01 degree and a zero check for every degree on each angle. The latter can also be used for correcting angular positions. The angular positions are continuously displayed using a five digit seven segment display for each of the four angles.

A schematic drawing of the motor-drive circuit is shown in figure 4. Each motor has a SCR controlled drive unit which enables the forward and the backward movements at two speeds, fast or slow. Three two-level signals (logical 1 or 0) are provided by three bits of a 12-bit flip-flop driver module (in the DIOS) for on/off, fast/slow and forward/backward control of each motor. The motor shaft is set in motion when the on/off bit is at logical level 1. The phase-shifted pulses— $V_G(F)$  for the fast and  $V_G(S)$

\*\*Fabricated in Nuclear Physics Division

†The digitizers manufactured by ECIL are based on an original design developed in the Reactor Control Division of BARC.

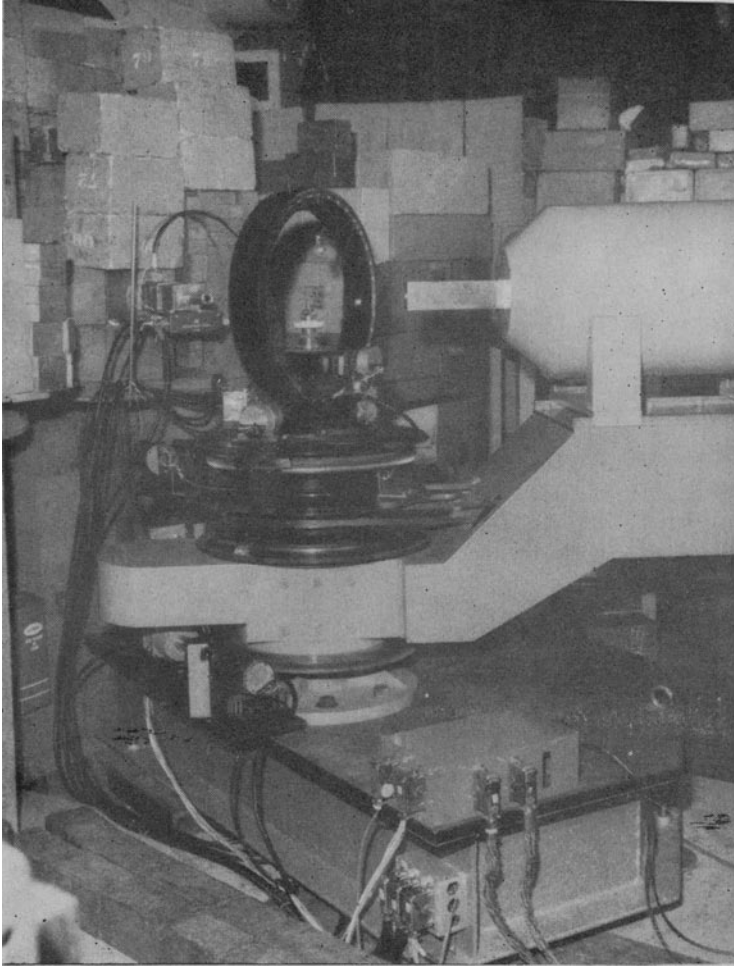


**Figure 3.** A photograph of the diffractometer

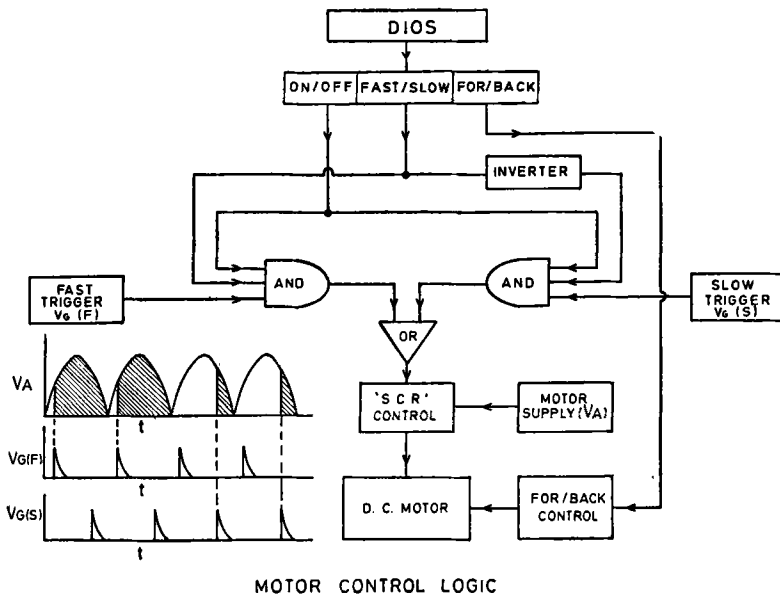


Figure 4. A schematic motor drive circuit

Table 2. Details of the drive systems

Drive	Motor Torque Lb-in	Gear Ratio	No. of pulses per rev. of digitizer	Setting speeds deg./min. Fast/Slow	Max. Over- shoot on Slow	Range in deg.	Accuracy* in deg.
$2\theta$	25	360 : 1	100	15 2	nil	-30 to 150	0.02
$\chi$	10	360 : 1	100	30 2	nil	-100 to 200	0.02
$\phi$	2	180 : 1	100 Stepped by 1 : 2 gear	40 3	0.01	$n \times 360$	0.03
$\omega$	10	360 : 1	100	15 2	nil	-60 to 60	0.02

\*The digitizers permit positioning accuracies of 0.01°. We must add to these the fabrication accuracies in the mechanical hardware. The overall accuracies, as estimated from measurements using standard crystals, then work out to around 0.02°.

for the slow modes—are applied to the SCR control gate depending on the level of the fast/slow bit. The supply voltage  $V_A$  (unfiltered) is applied to the armature winding of the motor through the SCR and to the field winding directly. The necessary phase shifts between  $V_A$  and  $V_G(F)$  or  $V_G(S)$  are generated using R-C phase shifters—phase shift for  $V_G(S)$  being much larger than that for  $V_G(F)$ . The forward/backward control is to be preset through a relay-contact commutator. Some details of the four angle drive systems are given in table 2.

#### 4. TDC-312 system configuration

The configuration of the TDC-312 computer system is shown schematically in figure 5. The DIOS is a real time peripheral device specially developed for exchange of information in digital form between the computer and the diffractometer. It operates under program control and can handle up to 256 functional modules, each having up to 12 individual digital controls. Each module has a unique address and is associated with one of the functions such as sensing data, transmitting data, response to contact interrupt or change of state, etc. and has its own decoder logic. The control of the diffractometer including the plotter, the visual display of four angles, the signal counts and the monitor counts involves about 22 functional modules which are listed in table 3. The bit allocation of two functional modules, viz., the control and the status registers, are illustrated in figure 6.

#### 5. Digital input/output subsystem (DIOS)

A schematic block diagram of DIOS alongwith one interrupting functional module is shown in figure 7. The DIOS interface controller generates seven different IOT instructions for enabling, disabling and interrogating the interrupt modules and for data transfer as listed in table 4. These instructions are derived by the instruction decoder by decoding the information available on bits 9-11 of MDR on the I/O bus, when the device selector is enabled by proper device address code (00011 for DIOS) on bits 4-8 of MDR. All address and data transfers to and from the accumulator are executed by these IOT instructions via the data and address gating circuits in the interface controller. To sense data in an input module or to load data in an output module, a load address (LAD) instruction which enables a specific module by loading the required address from accumulator into the DIOS address register (ADR) is

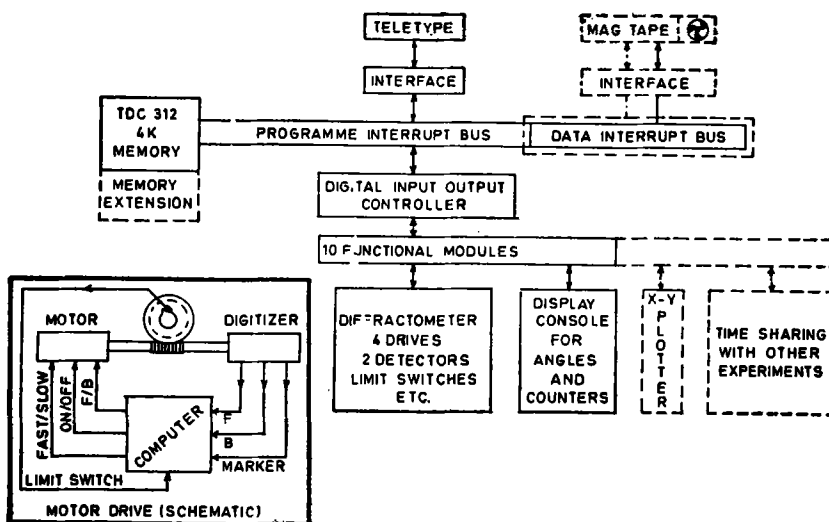


Figure 5. System configuration of the TDC-312 on-line controlled diffractometer

Table 3. Type and address of various functional modules

Function	Type of module	No. of modules	Address
Control register (for motors, shutters, etc.)	Flip-flop	2	304 305
Status register (for digitizers, limits, etc.)	Interrupt	2	301 302
Real time clock	Contact sense	3	307 310 311
Signal counter and display	Flip-flop counter	2	40 41
Monitor display	Flip-flop	2	56 57
Monitor prescaler	Flip-flop counter	1	303
Internal timer	Flip-flop counter	1	312
Four five digit angle displays	Flip-flop	8	42-47 54-55
X-Y plotter	DAC	1	317

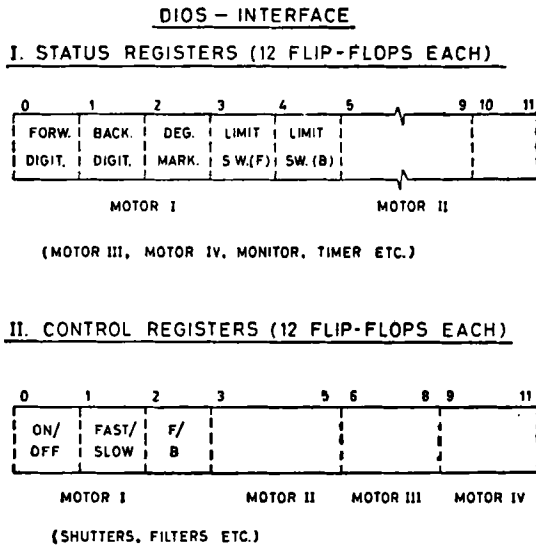


Figure 6. Bit allocation pattern of the control and the status registers

first executed. This is followed by a read data (RDT) or load data (LDT) instruction for transferring data from the module to the accumulator or the reverse.

The interrupt modules are monitored by an interrupt logic unit which sends an interrupt request to the computer whenever an interrupt flag is set. This request initiates the start scanner instruction (SSC) which enables the internal clock to increment the DIOS address register till it reaches the address of the interrupting module.

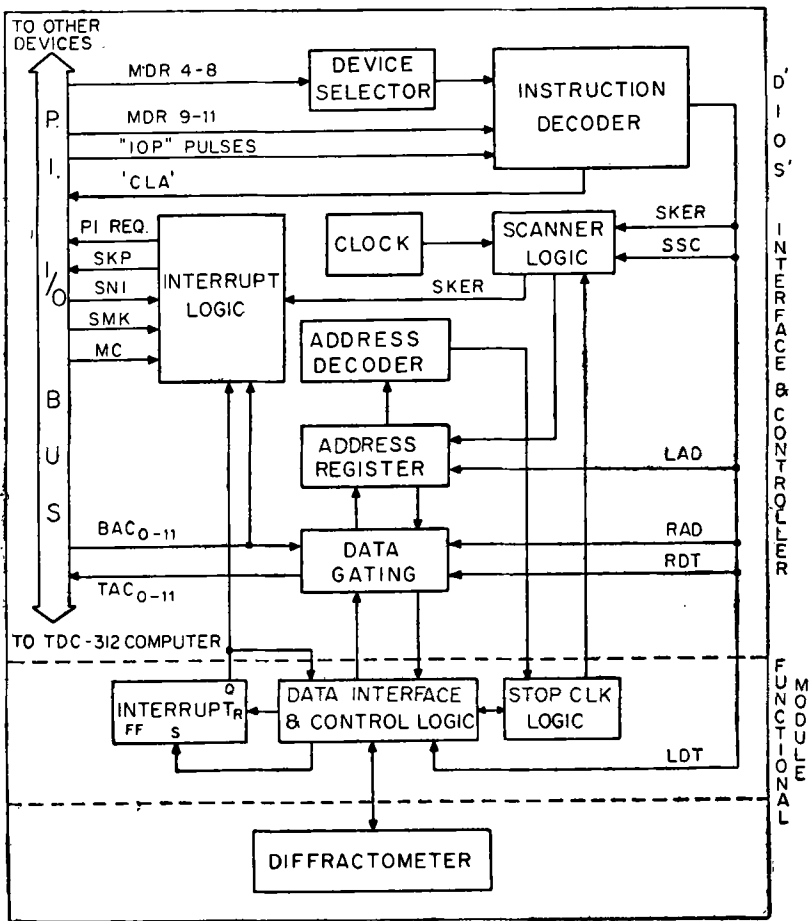


Figure 7. A schematic block diagram of the DIOS

Table 4. IOT instructions for DIOS

Instruction Code	Mnemonic	Description
6430	SNI	Skip next logical instruction of the program if DIOS is not interrupting
6433	SSC	Start scanning address of interrupting module
6431	SKER	Skip next logical instruction if scan flag is set (when the interrupting module is located) or skip next two instructions if watchdog flag is set (when the interrupt is spurious)
6436	LAD	Load 8-LSB's of accumulator into DIOS address register
6434	LDT	Store accumulator into the pre-addressed module
6435	RAD	Read contents of the address register into accumulator
6437	RDT	Read contents of preaddressed module into accumulator.

Table 5. Program for loading DIOS module through switch register

Program location	Code	Instruction	Comment
100	7403	ORS	Load module address from switch register (SR) into the AC (SR should be loaded with the address to start with)
101	6436	LAD	Select the address module in DIOS
102	7500	STP	Stop (for loading data into SR)
103	7403	ORS	Load data from SR into AC
104	6434	LDT	Load the data into addressed module
105	7500	STP	Stop

The address and the status of the interrupting module can be transferred sequentially to the accumulator using the read address (RAD) and the read data (RDT) instructions.

A typical program for loading data into a DIOS module for example is indicated in table 5.

## 6. System software

A compact 4K software package has been developed for automatic recording of 3-dimensional intensity data. It is essentially based on algorithms developed by Busing *et al* (1968) for use with the PDP-8 computer system. The routines have been extensively modified to suit the TDC-312 computer which, unlike the PDP-8, is a 4-bit opcode machine. The package mainly comprises of the following four sub-programs.

1. Arithmetic package—includes specially developed interpretive type floating point arithmetic routines.
2. Interface package—includes various device control and interrupt service routines.
3. Set-up package—includes routines for calculating the crystal orientation matrix given the cell parameters and the setting angles for two orienting reflections.
4. Data collection package—includes routines for recording 3-dimensional intensity data within the specified limits of indices and  $\sin \theta/\lambda$ .

Due to lack of sufficient memory capacity the last two programs had to be arranged in overlay as indicated in the memory map of the software in figure 8. A schematic flowchart of the system software highlighting the priority and sequence of interrupt handling is given in figure 9.

The motor drive routines are written such that all the angle destinations are approached by the shortest path, forward and backward. To prevent backlash and overshoot errors the final destinations are always arrived at in the forward slow mode. In the backward approach, this requires that the final destination be first overshoot by about a degree followed by reversal and slow forward reapproach. The average service times associated with the various interrupt service routines are listed in table 6. These do not include the overhead timing ( $\sim 40 \mu \text{ sec}$ ) associated with interrupt control function, saving of registers and device identification.

MEMORY MAP

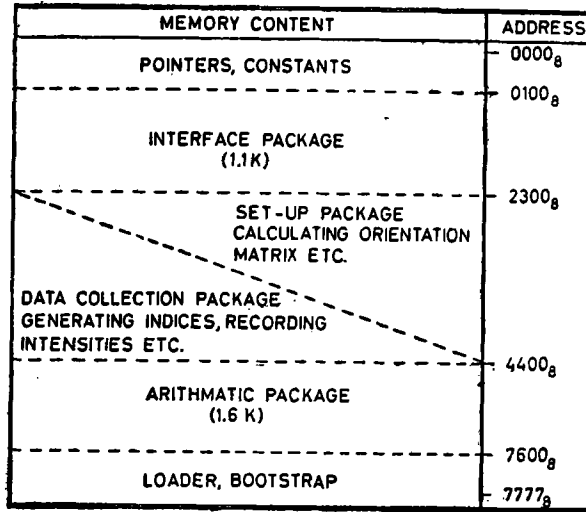


Figure 8. Memory map of the software package

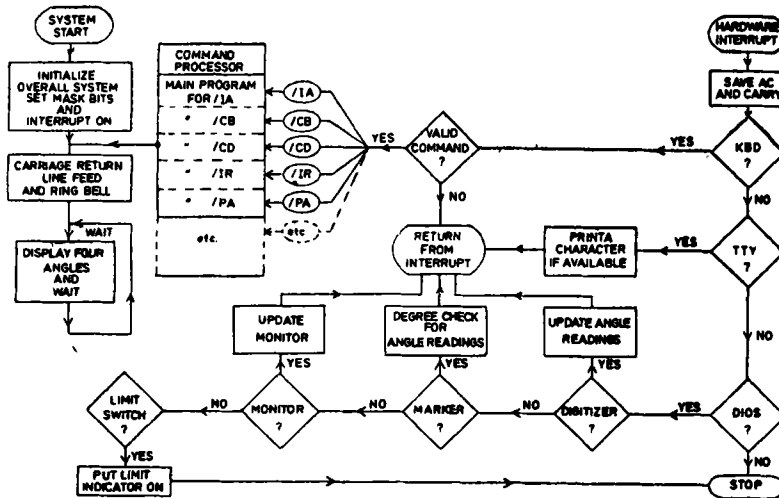


Figure 9. A schematic flowchart of system software for interrupt handling

Table 6. Interrupt service routing times (in  $\mu$  secs)

Digitizer	Updating monitor counter		TTY Printer		KBD Reader		
Update	135	Enable prescaler	80	Buffer empty	40	Illegal character	50
Update-slow	225	Disable prescaler	70	Buffer not empty	58	Command (/X <sub>1</sub> X <sub>2</sub> )	45
						1st CH. (X <sub>1</sub> )	50
						2nd CH. (X <sub>2</sub> )	80
Update-stop	185	—	—	—		Data character	52
Degree marker							
Correcting angle	60						

Table 7. The teletype commands

Command	Description	Data format <sup>(a)</sup>
<b>A. Initialisation commands</b>		
1. / <del>INIT</del>	Initialize the system	
2. /IT	Initialize angles at specified value	
	Initialize two theta	F 6.2
	/IC Initialize chi	"
	/IP Initialize phi	"
	/IO Initialize omega	"
3. /PA	Print all angles	—
4. /ZR	Read in zero angles of $2\theta$ , $\chi$ , $\phi$ and $\omega$	4F 6.2
5. /PZ	Print zero angles of $2\theta$ , $\chi$ , $\phi$ and $\omega$	—
6. /DT	Drive two theta to specified destination (initialization to be checked earlier)	F 6.2
	/DC Drive chi	"
	/DP Drive phi	"
	/DO Drive omega	"
7. /DM	Drive all motors to the specified destinations	4F 6.2
8. /PT	Print the current time	
<b>B. Set up commands</b>		
9. /CB	Compute crystal cartesian matrix (B) 7F7.4 given $\gamma$ and cell constants ( $\gamma$ , $a$ , $b$ , $c$ , $\cos \alpha$ , $\cos \beta$ , $\cos \gamma$ )	7F 7.4
10. /CU	Compute crystal orientation matrix (UB) given two orienting reflections: their $\omega$ , $\chi$ and $\phi$ (to be preceded by /CB)	2(313, 3F6.2)
11. /IA	Calculate setting angles for a given reflection hkl	313
12. /DA	Drive motors to calculated angles (to be preceded by /IA)	
13. /PM	Print and punch orientation matrix (UB)	
<b>C. Data collection commands</b>		
14. /RM <sup>(b)</sup>	Read matrix	Orientation matrix to be read through punched paper tape
		14
15. /IN	Initialize reflection number	
16. /CS	Clear all angle steps	
17. /ST	Step size for two theta	F 4.2
	/SC Step size for chi	"
	/SP Step size for phi	"
	/SO Step size for omega	"
18. /SD	Scanning data (A, B, N <sub>1</sub> , N <sub>2</sub> , Scan width = A + B × 2θ N <sub>1</sub> and N <sub>2</sub> = No. of left and right background steps)	2F4.2, 2I2
19. /SL	100* (sinθ/λ) minimum and maximum for data collection range	2I2
20. /IR	Scan individual reflection (given h, k, l)	3I3
21. /IS	Insert standard (No, repeat period and indices of standards)	2I2, 6I3
22. /CD	Start automatic data collection given h <sub>max</sub> , h <sub>min</sub> , k <sub>max</sub> , k <sub>min</sub> , l <sub>max</sub> , l <sub>min</sub> and indicator I (I=0, start from minimum indices; I=1, start from specified indices)	6I3, I1
23. /SR	Scan specified reflections (no. of reflections (N) and their indices)	I2, N(3I3)
24. /ID	Interrupt data collection	—
25. /RD	Resume data collection	—
26. /TY	Type comments	—

(a) Each individual data value must be delimited using either a space or a comma

(b) If 'Data collection package' is loaded without loading the SETUP package first.

The various software routines are interlinked and any individual routine can be initiated by sending an appropriate teletype command. There are in all over 40 teletype commands most of which are described in table 7, that enable free and easy dialogue between the user and the diffractometer and ensure a high degree of flexibility in the experiment.

## 7. Performance

The diffractometer has been calibrated using a standard crystal of KCl. The quality and the reproducibility of the intensity data recorded on-line are found to be extremely good. For example, the intensities of 54 reflections in an octant of the reciprocal space recorded using the KCl crystal refined to a conventional R-value of 1.5% on F. The reproducibility of the standard reflection intensities was within 2%. The average agreement factor between the intensities of equivalent reflections was somewhat higher at 3%. A careful examination of the individual agreement factors indicated the data to be suffering from significantly anisotropic secondary extinction effects. The variations in the intensities of equivalent reflections were suggestive of the type II kind of anisotropy (Coppens and Hamilton 1970). When the refinement was continued using the type II anisotropic extinction correction, it further converged to a surprisingly low R-value of 0.66% giving a very good individual agreement factor for all reflections. Application of the statistical half-normal probability plot test also showed the data to be free from any significant systematic errors. The derived values of the Debye-Waller factors for  $K^+$  and  $Cl^-$  ions were  $1.80(3) \text{ \AA}^2$  and  $1.86(3) \text{ \AA}^2$  respectively and the components of the tensor ( $W$ ) defining the anisotropy of particle size  $r = \lambda(N'WN)^{-\frac{1}{2}}$ , with respect to the cubic axes system were  $W_{11} = 29.9$ ,  $W_{22} = 98.5$ ,  $W_{33} = 210.7$ ,  $W_{12} = -7.6$ ,  $W_{13} = 26.0$  and  $W_{23} = -99.1$  ( $\text{micron}^{-2}$ ).

## Acknowledgements

We are grateful to Dr M Ramanadham for his assistance in diffractometer alignment and Dr P K Iyengar for his interest and encouragement.

## References

- Arndt U W and Willis B T M 1966 *Single Crystal Diffractometry* (London: Cambridge University Press)
- Arndt U W, Willis B T M and Casner R 1962 Report No. AERE-4143 (Atomic Energy Research Establishment, Harwell)
- Busing W R, Ellison R D, Levy H A, King S P and Roseberry R T 1968 Report No. ORNL-4143 (Oak Ridge National Laboratory, Oak Ridge)
- Busing W R and Levy H A 1967 *Acta Cryst.* **32** 457
- Coppens P and Hamilton W C 1970 *Acta Cryst.* **A26** 71
- Momin S N, Sequeira A and Chidambaram R 1974 *Indian J. Pure Appl. Phys.* **12** 121
- Willoughby T V, Marimoto C N, Sparks R A and Meyer E F 1974 *J. Appl. Cryst.* **7** 430